

Cloud Motions on Venus: Global Structure and Organization

SANJAY SHRIDHAR LIMAYE¹

Institute for Space Studies, Goddard Space Flight Center, NASA, New York, NY 10025

VERNER E. SUOMI

University of Wisconsin, Space Science & Engineering Center, Madison, WI 53706

(Manuscript received 7 April 1980, in final form 13 February 1981)

ABSTRACT

We present results on cloud motions on Venus obtained over a period of 3.5 days from Mariner 10 television images. The implied atmosphere flow is almost zonal everywhere on the visible disk, and is in the same retrograde sense as the solid planet. Objective analysis of motions suggests presence of jet cores (-130 m s^{-1}) and organized atmospheric waves. The longitudinal mean meridional profile of the zonal component of motion of the ultraviolet features shows presence of a midlatitude jet stream (-110 m s^{-1}). The mean zonal component is -97 m s^{-1} at the equator. The mean meridional motion at most latitudes is directed toward the pole in either hemisphere and is at least an order of magnitude smaller so that the flow is nearly zonal. A tentative conclusion from the limited coverage available from Mariner 10 is that at the level of ultraviolet features mean meridional circulation is the dominant mode of poleward angular momentum transfer as opposed to the eddy circulation.

1. Introduction

Atmospheric motions on Venus have been a target of scientific curiosity for over a decade now, since the first ground-based observations of cloud motions (Smith, 1967; Boyer and Guerin, 1969). Though several others have since observed such movements in ultraviolet images obtained from earth-based telescopes (Scott and Reese, 1972; Caldwell, 1972), observational difficulties have precluded a definition of the general circulation of the Venus atmosphere even at the cloud-top level until the Mariner 10, on its way to Mercury, encountered Venus in early 1974 (Dunne, 1974). In addition, Doppler shift measurements of spectral lines have yielded information about atmospheric motions on Venus (Traub and Carleton, 1975, 1979), although the coverage is sporadic.

Early Mariner 10 results on the Venus cloud motions were presented by Murray *et al.* (1974). Quantitative results obtained by interactive cloud tracking were presented by Suomi (1974)², and those obtained by stereoscopy, by Sidi (1976). All of these studies

were based on a somewhat limited number of images and gave only a general idea of the motions and their zonal and meridional dependence. A more comprehensive study to determine the atmospheric motions via cloud movements was undertaken by Limaye (1977)³ to determine the global circulation on Venus from the images at the cloud-top levels. The vortex organization suspected by Murray *et al.* (1974) and by Suomi (1974)² was evidenced in this study through a polar space-time composite of several Mariner 10 ultraviolet images (Suomi and Limaye, 1978). In this paper we present the quantitative part of that study which indicates the spatial structure of the atmospheric motions on Venus during the Mariner 10 encounter.

The terms "clouds" and "contrast features" are used synonymously in this paper and this dual usage reflects our poor knowledge of what those contrasts are due to. Nevertheless, it is an implicit assumption that the movements of the clouds seen in Mariner 10 images are equivalent to atmospheric motions.

2. The data

The Mariner 10 spacecraft carried two television cameras (Dunne, 1974). Together they returned over

¹ Present affiliation: University of Wisconsin-Madison, Space Science & Engineering Center, 1225 W. Dayton Street, Madison, WI 53706.

² Suomi, V. E., 1974: Cloud motions on Venus. *The Atmosphere of Venus*, Proceedings of a conference held at the Goddard Institute for Space Studies, New York, 15-17 October, 1974, J. Hansen, Ed., NASA SP-382.

³ Limaye, S. S., 1977: Venus stratospheric circulation: A diagnostic study. Ph.D. Thesis, University of Wisconsin-Madison.

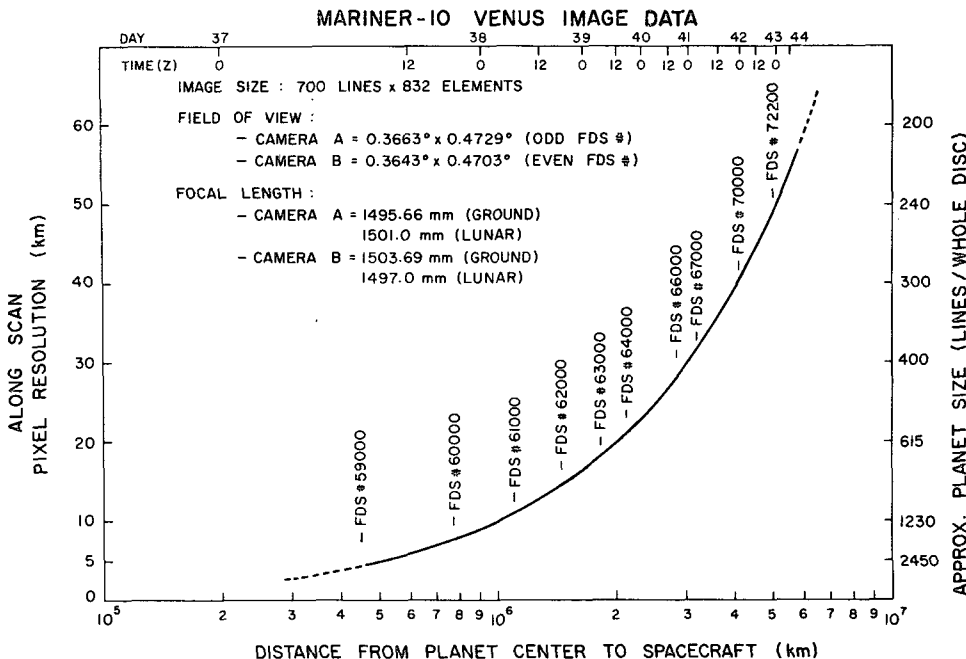


FIG. 1. Montage of selected Mariner 10 ultraviolet images of Venus, showing the variation in spatial resolution.

3400 useful images of Venus, mostly in solar reflected ultraviolet light (Murray *et al.*, 1974, Anderson *et al.*, 1978). The final destination of Mariner 10 was Mercury and the trajectory selected resulted in a fly-by approach to Venus from the night side. After a gravitational assist from Venus, the spacecraft proceeded toward Mercury for three successful encounters. It was on this outbound asymptote that the images were obtained for approximately eight days. Fig. 1 shows a sample of the images obtained. The size of Venus is seen to decrease as the spacecraft receded from Venus. This is also indicated quantitatively in Fig. 2 wherein the pixel size at the sub-spacecraft point as well as the size of the planet in terms of image scan lines per whole disk are shown as a function of the distance of the spacecraft from Venus center. Also shown in this figure are the Flight Data System (FDS) numbers that incremented for each image at 42 second intervals. The FDS number is thus a unique way of identifying a Mariner 10 image. The images used in the present work are listed in Table 1 along with the corresponding pixel sizes at the sub-spacecraft point.

The phase angle of the planet, i.e., the angle between the sun, the center of the planet and the spacecraft, varied gradually from 30°/24°, thus the choice of images for tracking features was governed solely by their spatial resolution and the elapsed time. Primarily only full disk or near full disk images were used in this study because the navigation of these images is simpler. The images

were corrected for the geometric and photometric distortions caused by the television camera; however, the reseau marks seen in the images were deliberately not removed as they were used to determine the camera characteristics. The bulk of this pre-processing was done at the Image Processing Laboratory of the Jet Propulsion Laboratory (JPL).

The object of the present study was to study the atmospheric motions as revealed by ultraviolet feature motions over as much of the planet and for as long a period as possible. No direct measurements on the night side of the planet are possible since the images were taken in solar reflected ultraviolet light. However, in view of the fact that the upper atmosphere of Venus moves at roughly 100 m s⁻¹, in less than 4 days the entire upper atmosphere rotates into the field of view of the Mariner 10 cameras. Thus, despite the fact that only about half of the atmosphere is visible at any given instant, the movements can be longitudinally stratified in terms of relative longitude that covers the entire atmosphere. This is analogous to constructing a spatial field from a time history of meteorological data from a few stations; temporal resolution is exchanged for spatial coverage. This procedure allowed us to study the variation of the zonal component of motion of the ultraviolet features as a function of relative longitude as shown below. Previously, we have used this procedure with a semi-empirical model for the meridional dependence of the zonal mean zonal component of the wind to look for planetary waves, and indeed

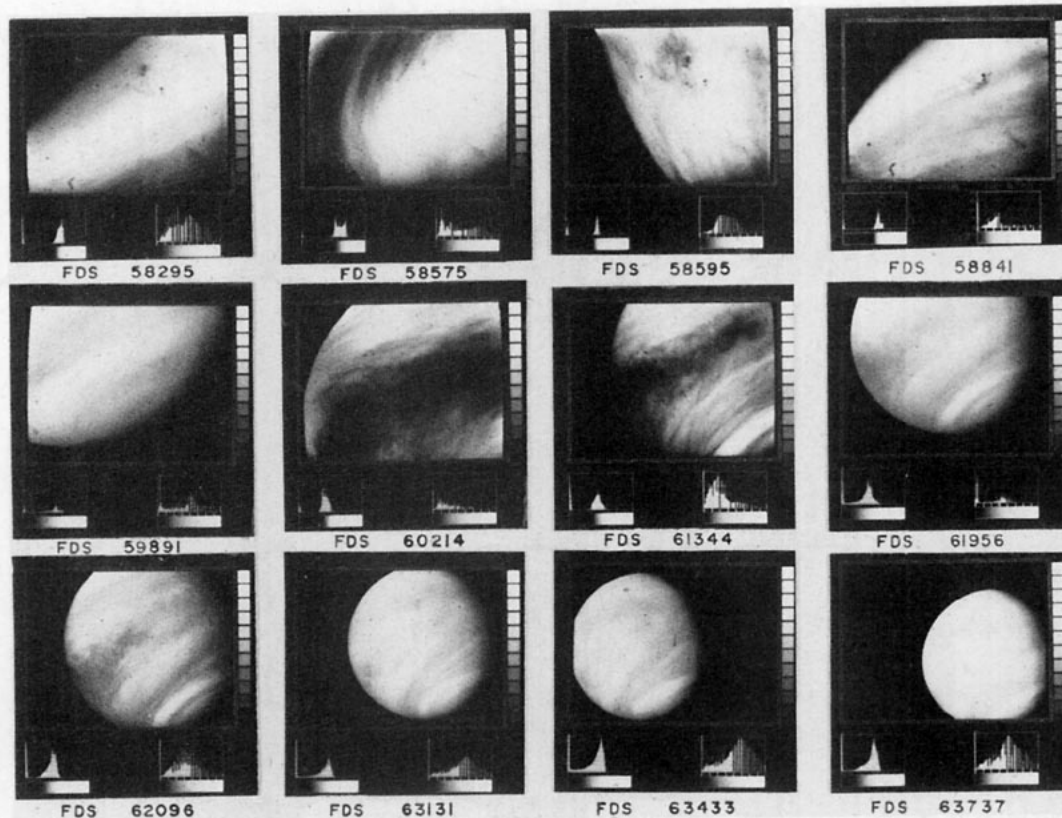


FIG. 2. Range of image resolutions obtained at Venus from Mariner 10. The Flight Data System (FDS) numbers increment at 42 s intervals and are used to tag individual images sequentially, and are indicated at various times after closest approach. Approximate size of Venus in terms of image scan lines is indicated by the scale on the right.

the existence of a planetary wave of wavenumber 1 was indicated in that analysis (Limaye and Suomi, 1977).

3. The technique

a. The mechanics of tracking

The corrected images were displayed on a special purpose image processing device called McIDAS (Man computer Interactive Data Access System) designed and built at the Space Science and Engineering Center (SSEC) of the University of Wisconsin-Madison. A description of this system, which is ideally suited for cloud-tracking, has been given by Chatters and Suomi (1975).⁴ The images were navigated, i.e., the forward and backward transform relationships between the coordinates of a particular feature seen in a given image and the Venus coordinates of the same feature, were determined for each image from the knowledge of the

Venus ephemeris and the trajectory of the Mariner 10 spacecraft. The navigation procedure involves determination of the sub-spacecraft point in the image as there are no "landmarks" visible in these images. Due to the large focal length of the television cameras (1500 mm) the spacecraft was more than a million km away from Venus when these images were shuttered. Hence the sub-spacecraft point on Venus coincides with the center of the disk. Knowledge of the orientation of the cameras and the location of the sub-spacecraft point in the image is sufficient to determine the Venus coordinates of any point in the image.

Navigated images were aligned and displayed as a time sequence on successive frames of the McIDAS display. The ultraviolet markings seen in the images were visually selected and followed in at least three images at a time. A latitude and longitude grid generated for each image ensured proper registration of the successive images; however, it was not normally displayed to prevent any operator bias in tracking. The computer that governs the McIDAS display is programmed to access the digital brightness data corresponding to the target feature in two successive images and, using one of several pattern

⁴ See also Smith (1975). See Suchman and Martin (1976) for a study of accuracy and reproducibility of tracer winds on earth on this system.

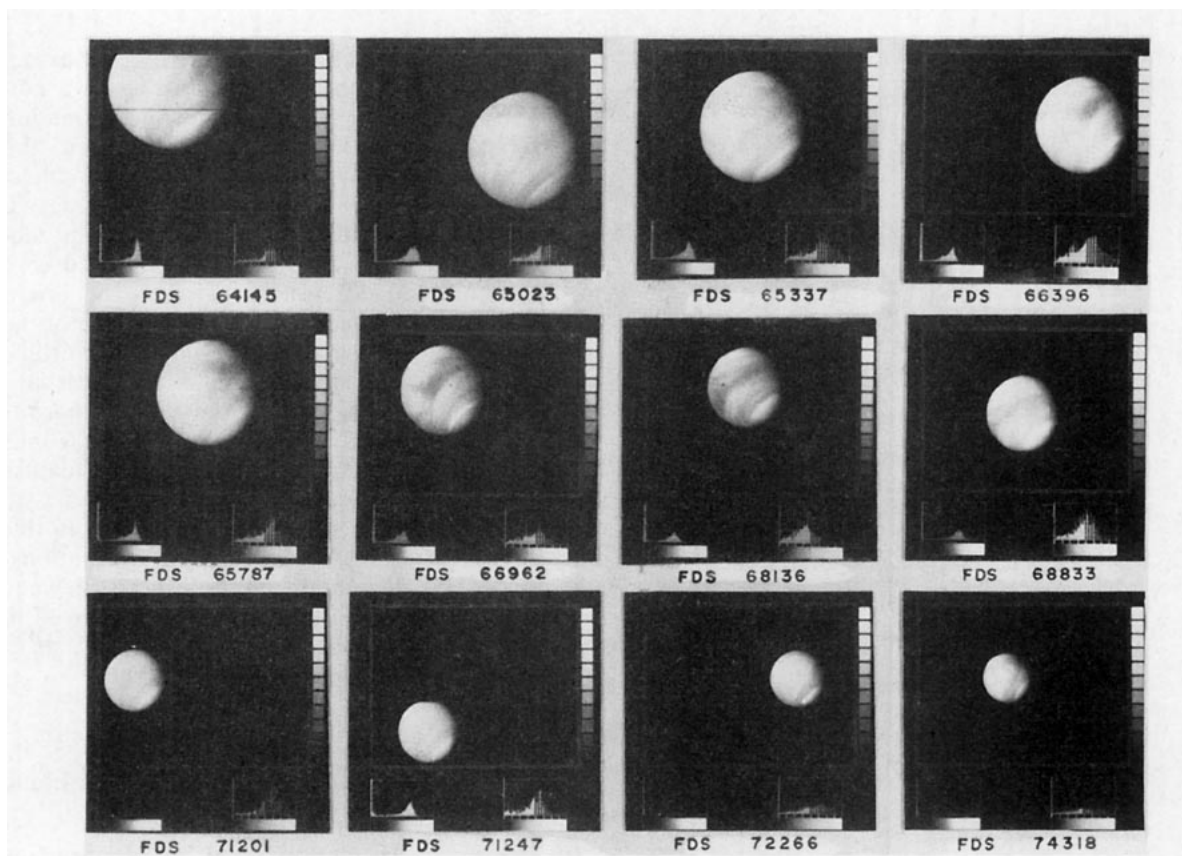


FIG. 2. (Continued)

recognition techniques, to obtain an estimate of the target location in the second image. The metric used for such digital tracking is usually the straight cross-correlation matrix (Smith and Phillips, 1975); however, other approaches, such as looking for brightness gradients within the feature, etc., are possible.

Manual tracking, i.e., when the operator determines the locations of a feature in successive images, is also available on McIDAS. This approach, which is more useful when well-defined features are available, was used for tracking, but only infrequently. Previous work had shown that the differences between the manually tracked vectors and the digitally tracked vectors were small (Suomi, 1974).³

At high latitudes few trackable features were usually seen, thus precluding any measurements. However, visually it was possible to sense the general nature of the motions when polar projections of the images were displayed as time-lapse sequences on McIDAS. A similar situation existed for images taken later in the Mariner 10 observing period, when the image resolution was poor and the time interval between images was large. In this instance also it was possible to visually monitor the movements of the ultraviolet features although, once again, very few successful measurements were possible.

b. Feature selection for tracking

Extreme care was taken in the selection of the contrast features as tracking targets to ensure the validity of such tracers as indicators of true atmospheric motion and that no contamination occurred due to propagating waves. For example, no targets were selected within the circumequatorial belts (CEB), that were measured to move (always from north to south) at $\sim 20\text{--}40\text{ m s}^{-1}$, and which surely do not correspond to atmospheric mass motion.

In digital tracking, the target areas were usually between 12×12 and 24×24 pixels depending on the pixel size on the planet. This corresponds to dimensions of approximately between 200×200 and 600×600 km. By terrestrial standards these are very large features indeed. In the Venus images however, these are about the smallest isolated features that can be tracked over a period of a few hours. In higher resolution images the contrast features are extremely diffuse, and need to be tracked over much shorter periods. In order to allow a study of any relationship between brightness, size and texture or contrast of features and their motions, the average brightness of the targets, their size in pixels and the standard deviation of the target brightness were recorded along with positions. No systematic

TABLE 1. Mariner 10 images used in the study.

FDS no.	Shutter time (day hh:mm:ss)	Spacecraft range (km)	Pixel size at image center (km)	Phase angle (deg)
61338	038 10:17:57	1 233 795	12.2	29.8
61360	10:33:21	1 247 503	12.4	29.8
61486	12:01:34	1 284 827	12.7	29.7
61496	12:08:33	1 288 275	12.8	29.7
61648	13:54:57	1 340 685	13.3	29.7
61788	15:32:57	1 388 958	13.8	29.6
61786	15:31:33	1 388 268	13.8	29.6
61954	17:29:09	1 446 197	14.3	29.5
62080	18:57:21	1 489 644	14.7	29.4
63601	039 12:42:03	2 014 368	19.9	28.6
63737	14:17:14	2 061 320	20.4	28.5
63903	16:13:26	2 118 638	21.0	28.4
64289	20:43:38	2 251 964	22.3	28.2
64747	040 2:04:14	2 410 250	23.9	27.9
64897	3:49:14	2 462 113	24.4	27.8
65023	5:17:26	2 505 675	24.8	27.7
65173	7:02:26	2 557 561	25.3	27.6
65317	8:43:14	2 607 384	25.8	27.5
65485	10:40:50	2 665 527	26.4	27.4
65627	12:20:14	2 714 685	26.9	27.3
65787	14:12:14	2 770 090	27.4	27.3
65923	15:47:26	2 817 198	27.8	27.2
66067	17:28:14	2 867 090	28.3	27.1
66223	19:17:26	2 921 155	28.9	27.0
66380	21:07:19	2 975 585	29.5	26.9

dependence of the motions on the brightness of the features was obvious globally. Locally, curious variations in the velocities were frequently seen that could best be explained by vertical shear of the wind equal to meters per second per kilometer. In several instances, thin, filmy cloud material could be observed to move over the ultraviolet features, and this gave further credence to suggestions of vertical shear of the horizontal motions, although no measurements were possible.

Ideally, isolated small features should be chosen for tracking, but this is not always possible in the Venus images where the features appear very diffuse. In general, edges of features were not selected for tracking, except when no other targets were available in the vicinity. The rationale for this strategy follows from an analogy with the expanding anvil of a terrestrial deep cumulus congestus, or that of an active tropical cloud cluster: the edge displacements are more an indication of the evolution of the cloud system rather than the movement of the cloud itself.

We do not as yet know the origin of the contrasts on Venus, and though their cause is unimportant for tracking purposes, it is important to know if there is any peculiar quality of the features that would preclude their use as indicators of atmospheric motion. Time lapse movies generated from

the Mariner 10 images however were quite convincing, at least for us, that the contrast feature motions show a well organized atmospheric motion field.⁵ No systematic difference between the motion fields of the "bright" and the "dark" ultraviolet contrast features is obvious from the images. This does not preclude any differences in the motions of such features that may be associated with any slight altitude differences between the bright and the dark ultraviolet features. The wealth of the data indicates that there cannot be large vertical variations in the "cloud tops" of bright and dark features (Travis, 1975). Thus even though there is evidence for vertical wind shear in the Venus atmosphere, its magnitude as shown by UV feature motions on a local scale is small compared with the large zonal flow. No attempt was made in this work to study any local variations in the motions, and no explicit distinction is made here between the movements of the dark features as opposed to those of the bright features. However, in practice, predominantly bright features were tracked.

c. Quality control of measurements

The error in a single determination of cloud velocity is due to several causes:

(i) The image resolution (~ 20 km) determines the precision with which the planetary coordinates of the feature can be determined, and this coupled with the time interval between the images (~ 90 min) gives an inherent uncertainty in the velocity (~ 4 m s⁻¹).

(ii) Navigation errors limit the accuracy with which the planetary coordinates of the feature can be determined, given its image coordinates.

(iii) Random error in locating a feature in successive images in either the manual tracking mode or the digital tracking mode.

(iv) Operator error in selecting and identifying a feature being tracked.

The first two error sources can be controlled to a large extent and care has to be taken to minimize those due to the latter two sources. In the case of digital tracking the error due to misidentifying a feature in the second image is minimized by looking at the two-dimensional field of cross-correlation coefficients and looking for well defined maxima. Any vectors which have correlation peaks on boundaries of data and those with secondary or multiple peaks are rejected. In manual tracking no such criterion is available for quality control, and thus the acceptance or rejection of questionable targets is a matter of operator judgement.

⁵ Copies of the time lapse sequences are available in the form of 16 mm color movies and as video cassettes.

The last error source, total misidentification of a feature, can be controlled by proper selection of the time interval between successive images. Attention has to be paid to the physical scales of the features being tracked, the general morphology of features in the vicinity of the feature, and, most importantly, the evolution time scale of the feature. For example, in the vicinity of the sub-solar region, cellular features that mimic deep convective clouds, have typical life times of only a few hours (Murray *et al.*, 1974; Belton *et al.*, 1976). Thus new features develop in regions close to where the old ones have decayed, and can be mistaken to be the same feature. One remedy for this type of error was to monitor the images taken between the ones being used for tracking, or to use finer time resolution for tracking when feasible.

One possible approach to controlling the number of "bad" measurements is to require a consistency between the first and the second vector obtained by tracking a feature over three consecutive images. In the present study the elapsed time between the first and the last image of a triplet was generally about three hours, thus the features would move only about 10 to 15 degrees in longitude over this period, and no large accelerations are expected over this space and time interval. The two vectors obtained by tracking a feature over the three images in a triplet were flagged as erroneous if they differ in magnitude by, say, 20 m s⁻¹ in either component of motion.

The error in a single vector due to the first two sources mentioned above is not greater than ~5-6 m s⁻¹. This was controlled by proper choice of images and intervening time intervals (all the images in a triplet were chosen to be from the same camera to minimize any errors due to systematic image distortions) and careful navigation so that the displayed sequence was aligned as accurately as possible.

4. The results

a. Spatial coverage

Uniform global coverage of cloud motions is highly desirable, but this is not entirely feasible in the present case due to the Mariner 10 trajectory and the duration of the Venus encounter observation period. All of the images used for tracking features show Venus in an oblique perspective view with the center of the image corresponding to about 19 degrees south latitude. The southern hemisphere of the planet is thus seen better and hence sampled better in the data. Decreasing solar illumination away from the sub-solar point and accompanying lack of sufficient detail make finding trackable features, compared with terrestrial images, a very difficult task indeed. This is particularly true at high latitudes near and within the bright polar cloud in both hemispheres,

and very little coverage is obtained in terms of motions.

Despite these difficulties, over 2000 high quality vectors were obtained in a wide range of planetary latitudes and longitudes. The sampling statistics in terms of latitudinal and longitudinal coverage are summarized as histograms in Fig. 3. The central regions of the images are obviously sampled more often than other regions as is evident in the figure.

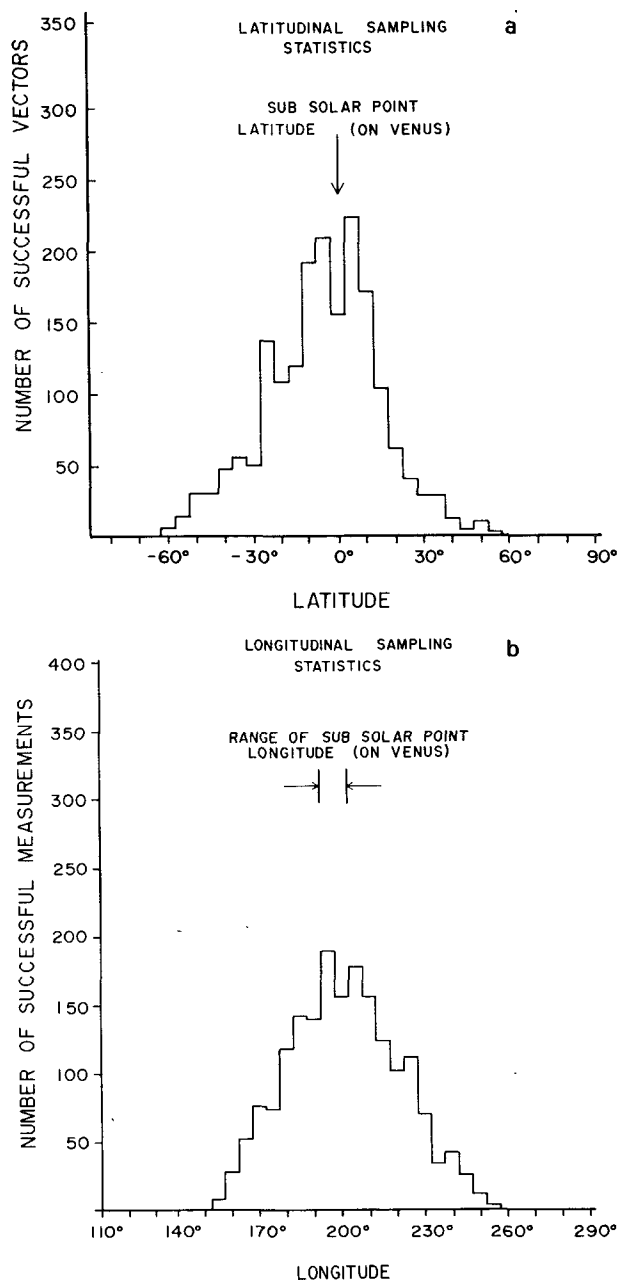


FIG. 3. Spatial coverage of the ultraviolet features tracked: (a) histogram of UV feature latitudes, (b) histogram of UV feature longitudes.

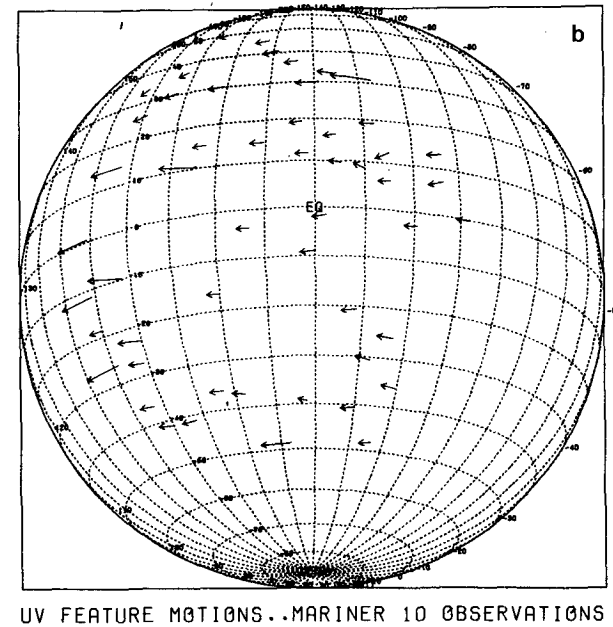
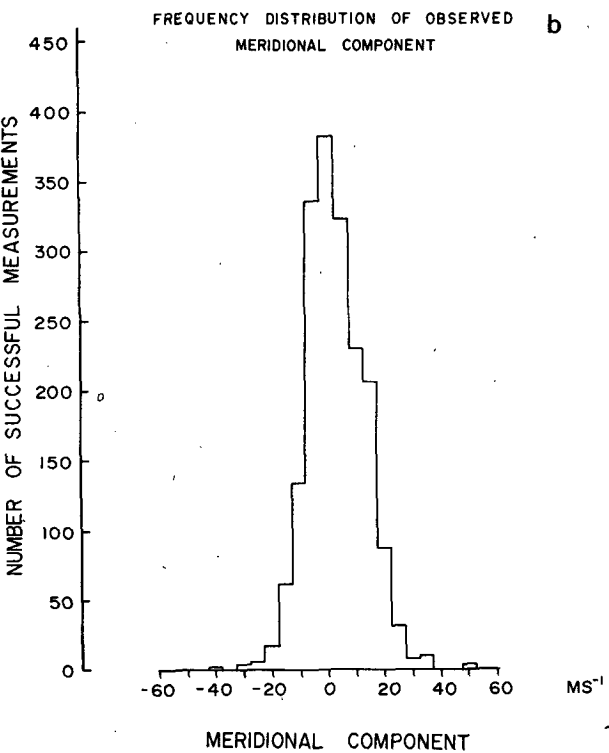
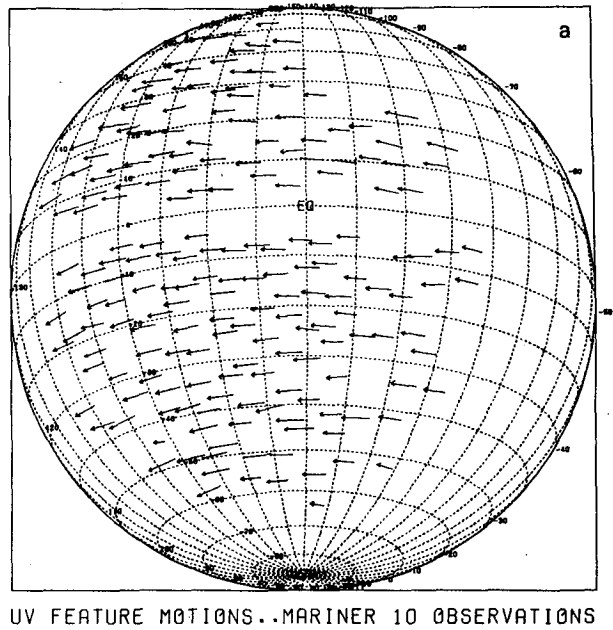
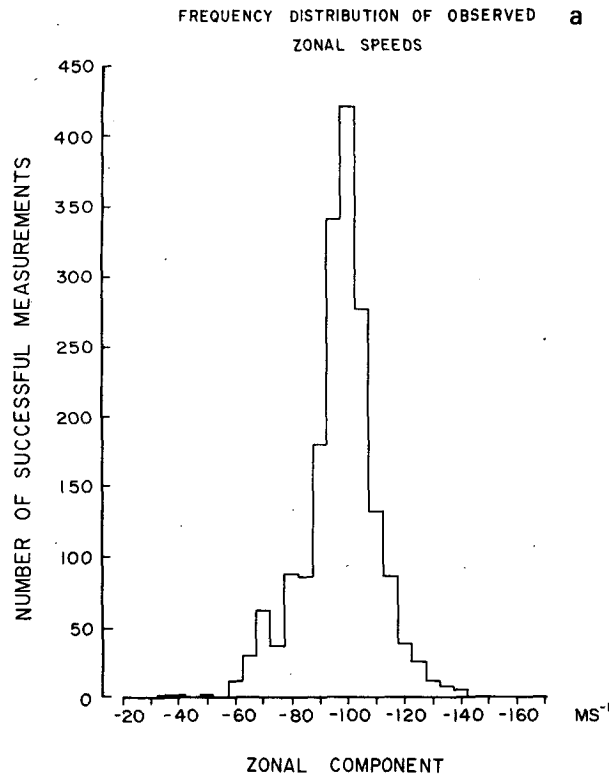


FIG. 4. Observed UV feature velocities: (a) zonal component, (b) meridional component.

FIG. 5. Orthographic view of the measured vectors: (a) "normal" vectors, and (b) "abnormal" vectors that deviated by more than two standard deviations from the local mean values. The length of the arrows indicates the magnitude of the speed and they point in the direction of UV feature movements.

The sub-solar point moved from $\sim 190^\circ$ longitude to $\sim 200^\circ$ longitude and this region was also well sampled. The measured zonal and meridional speeds for all targets also are shown as histograms in Fig. 4.

About 7% of the vectors were found to depart from zonal mean values for either the zonal component or the meridional component of motion by

more than two standard deviations. Of these "abnormal" vectors, ~30% showed a faster zonal component than the local average. It is quite possible that these abnormal vectors represent wave phenomenon superposed on the general flow field. Due to their small number, no further analysis was performed. Both the "normal" vectors and "abnormal" vectors are shown in the same oblique orthographic projection of the images in Fig. 5. For legibility, overlapping vectors have been box averaged. The arrows point in the direction of the movements of the ultraviolet features, while their relative magnitude is represented by the length of the arrows. In both cases the dominant zonal nature of the flow is evident.

b. Spatial structure of the motions

Terrestrial atmospheric flow is quite variable in time and in space, and the same may be expected on Venus. In the present case, however, the temporal coverage is limited to ~4 days and is not long enough to meaningfully analyze temporal variations in motions as discerned from the movement of the ultraviolet clouds. In addition, the measurements obtained are not homogeneous in terms of horizontal scale—earlier in the image sequence the resolution is greater than that nearer the end of the sequence and hence the size of the features used for tracking is larger near the end of the sequence. However, as the original goal was to obtain the global coverage of motions, such differences were ignored, and the results from all the image triplets were analyzed together to determine the spatial structure only. Thus, the net result is that of both temporal and spatial smoothing on a local scale. The advantage is that the results can be stratified in longitude relative to a certain reference point such as the semi-permanent, recurring dark Y feature, and a near global (longitudinal) view of Venus may be obtained as shown below. The analyses with respect to Venus longitude may then be viewed as being time averaged fields over the observation period of ~3.5 days, and the dark-Y-relative longitude results may then be interpreted as an "instantaneous" global field as the images allow measurements to be made only in the sunlit hemisphere. The two-dimensional spatial structure of the motions is presented next and zonally averaged profiles are discussed later.

c. Grid-point analysis of the motions

The density of the vectors in 5° latitude by 5° longitude squares was found to be sufficiently high in terms of both the Venus coordinates as well as over most of the dark-Y-relative longitudes; hence, a grid-point analysis was performed to reveal the two-dimensional structure of the motions. Restriction

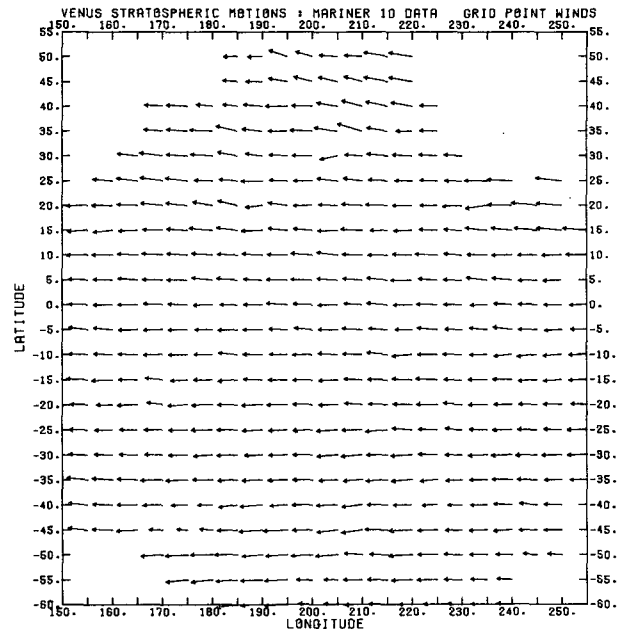


FIG. 6. Objective analysis of the results.

were placed on the minimum number of vectors used for interpolation (>5), and the search or the interpolation radius (<5 degrees in latitude and longitude).

The resultant motion field is depicted in Fig. 6 in terms of body-fixed Venus coordinates with the length of the arrows proportional to speed and the direction corresponding to direction of the flow. The near zonal nature of the motions is evident, but due to the smallness of the meridional component the smaller scale details cannot be clearly seen. The details can be seen better in separate isotach analyses of the zonal and meridional components.

d. Zonal component: Isotach analysis

Figs. 7a and 7b show isotach analyses of the objectively analyzed zonal component of motion for Venus longitudes and dark-Y-relative longitudes, respectively. Near the corners of the figure coverage is not sufficient to perform an adequate analysis. The shaded regions have a zonal component faster than 100 m s^{-1} , and contours are drawn every 10 m s^{-1} . The magnitude of the zonal component is between 90 and 100 m s^{-1} over most of the longitudes in the equatorial latitudes, with small pockets of somewhat slower and faster zonal speeds between 210° longitude and 240° longitude. Within the longitude range 190 – 200° the zonal component shows peak magnitudes greater than 120 m s^{-1} near 40° north latitude, and over 100 m s^{-1} near 45 – 50° latitude in the southern hemisphere. Zonal com-

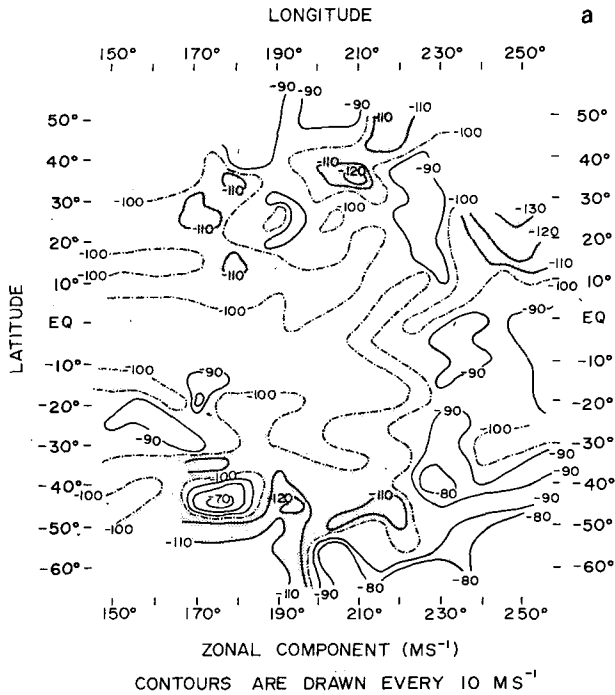


FIG. 7a. Isotach analysis of the zonal component with Venus longitudes.

ponents faster than 130 m s^{-1} are evident near the morning terminator at $\sim 30^\circ$ north latitude. A somewhat slower zonal component maximum is observed in the southern hemisphere between 40 and 50° latitude and centered at $\sim 173^\circ$ longitude.

The dark-Y-relative longitude map also shows the same meridional structure since only the longitudes are different, and the longitudinal structure shows faster zonal speeds at relative longitudes ranging from ~ 310 to at least 340° longitude and also be-

tween ~ 100 to 160° . Two regions akin to terrestrial jet cores are seen in the southern hemispheres with core zonal speeds faster than -110 m s^{-1} between 40 and 50° and at longitude regions centered approximately at 210° and 290° . Existence of similar regions is also suggested in the northern hemisphere with somewhat higher peak zonal speeds. The dark-Y-relative longitude structure over the observed range is suggestive of slower and faster flow in low latitudes as would be expected in a planetary wave. It is consistent with the earlier result wherein a semi-empirical meridional profile model was used to bring out the systematic variation of the zonal speed at the equator with longitude (Limaye and Suomi, 1977).

The isotach analysis of the zonal component of motion shows that the mean zonal component increases with latitude and the superimposed eddy components have magnitudes between 10 – 20 m s^{-1} . Note that the phase relationship of the eddies is better preserved in the Y-relative longitude map compared to the planet longitude map due to the time averaging.

e. Meridional component: Isotach analysis

The isotach analysis of the meridional component of motion as obtained after objective analysis is presented in Figs. 8a and 8b (for planet and dark-Y-relative longitudes, respectively). In these figures, shaded regions indicate a negative meridional component. Normal meteorological convention is used for measuring direction, so that a positive meridional component in the northern hemisphere, and a negative meridional component in the southern hemisphere correspond to poleward motions. The dominance of the shaded regions in the southern latitudes and the lack thereof in the northern hemisphere

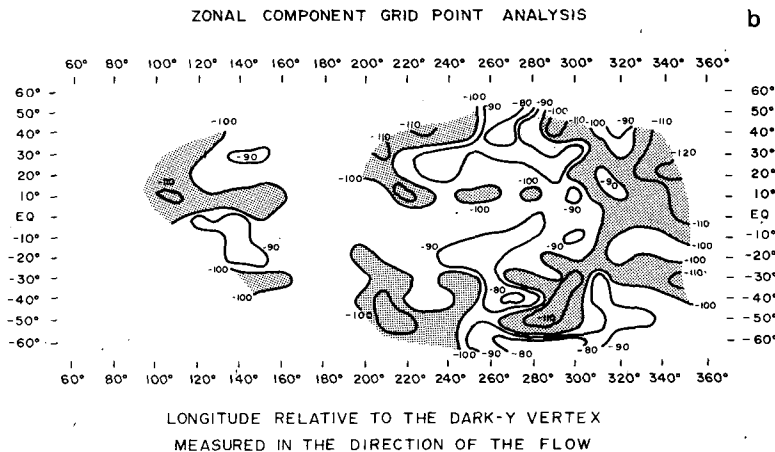


FIG. 7b. Isotach analysis of the zonal component with reference to the dark-Y-relative longitudes.

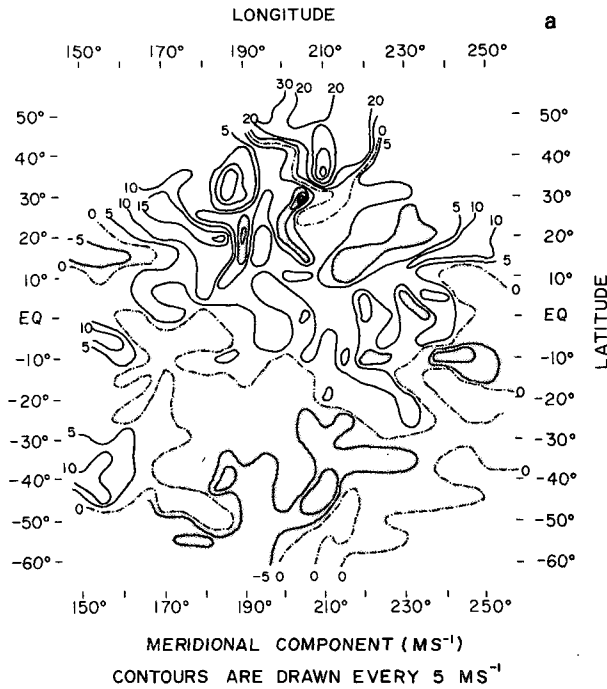


FIG. 8a. Isotach analysis of the meridional component with Venus longitudes.

immediately leads to the conclusion that the motions are directed predominantly towards higher latitudes in both the hemispheres.

The dark-Y-relative longitude meridional flow field naturally shows the same meridional structure, and the longitudinal structure is suggestive of both large and small scale eddies. Visually, the field appears correlated with that of the zonal component as can be ascertained by overlaying one over the other, although as yet we have not sought to calculate it directly except in a zonal mean sense.

The magnitude of the meridional component at all observed latitudes and longitudes is quite small compared to the zonal component. In equatorial latitudes, meridional speeds are generally less than 10 m s^{-1} . In the northern hemisphere there is a pronounced tendency for the meridional component to increase with latitude, reaching values exceeding 30 m s^{-1} beyond $\sim 30^\circ$ latitude in isolated regions. The same general increase appears to occur in the southern hemisphere also, albeit to a lesser degree. Isolated regions of higher and lower components are scattered at all latitudes similar to those found in the zonal component analysis. Such local minima and maxima in the zonal and meridional component appear to be related, though exact phase relationships have not been analyzed and are not presented here. Their existence alone suggests the spatial variability of motions and provides rough limits on variability. Such variations can occur due to the existence of both coherent and incoherent processes in the Venus atmosphere. Inertial effects have been suggested to occur in the Venus atmosphere (Limaye, 1977; Rossow and Williams, 1979), and may be one cause of such variability.

f. Zonally averaged profiles

It is interesting to determine the zonally averaged profiles of the motions to study the atmospheric circulation. In the present case, the zonal averages are naturally restricted to the observed longitudes, and hence the averages determined are biased estimates. With this in mind, the results were stratified in several latitude intervals and the averages and standard deviations determined. The resultant profiles for the zonal component, the corresponding angular speed, and the meridional component are shown in Figs. 9, 10 and 11 respectively. Also shown in Figs. 9 and 11 are the standard deviations about

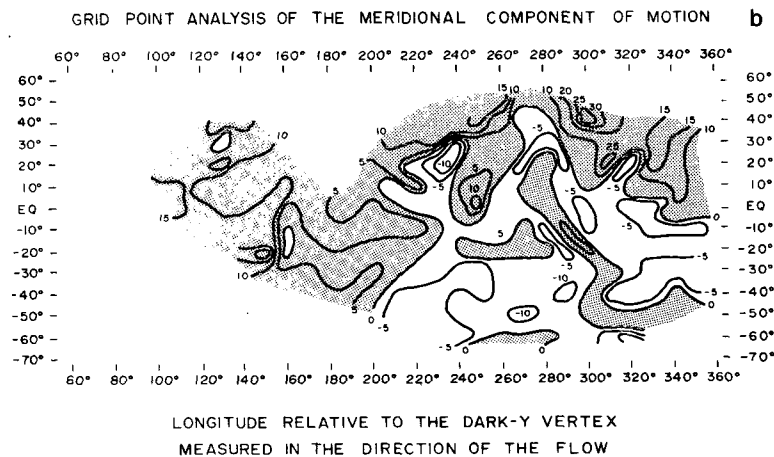


FIG. 8b. Isotach analysis of the meridional component with reference to the dark-Y-relative longitudes.

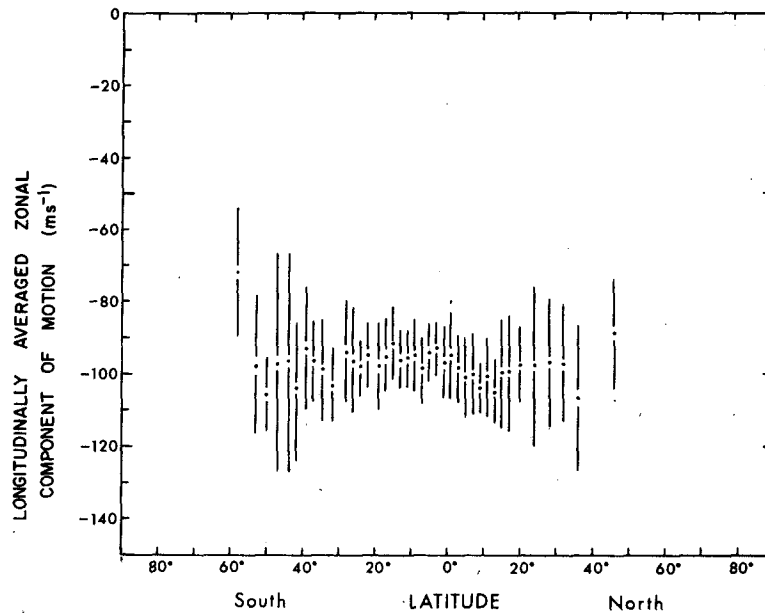


FIG. 9. Latitudinal profile of the space-time-averaged zonal component of motion of the UV features.

the mean values in each latitude interval (the length of the vertical line above and below the point is equal to one standard deviation). The standard error, defined as the standard deviation divided by the square root of the number of observations in a latitude bin, is less than 2 m s^{-1} for both the components in low and mid latitudes (-35 to $+25^\circ$), and somewhat higher at high latitudes.

The longitudinally averaged zonal component over the entire observation period shows the same shape that was reported by Suomi (1974). From an equatorial mean value of $\sim -97 \text{ m s}^{-1}$, the mean zonal component increases to -108 m s^{-1} at $\sim 50^\circ$

latitude in the southern hemisphere, and at $\sim 38^\circ$ latitude in the northern hemisphere. Polewards of these latitudes, a sharp decrease in the mean zonal component is seen, although there are few observations at very high latitudes. The variability of the zonal component appears to be somewhat greater at higher latitudes than at lower latitudes. However, how much of this variability is due to uneven sampling and foreshortening problems and how much is real is unknown.

This profile of the zonal component is certainly not a solid body rotation profile in which the mean zonal component would fall off as the cosine of the

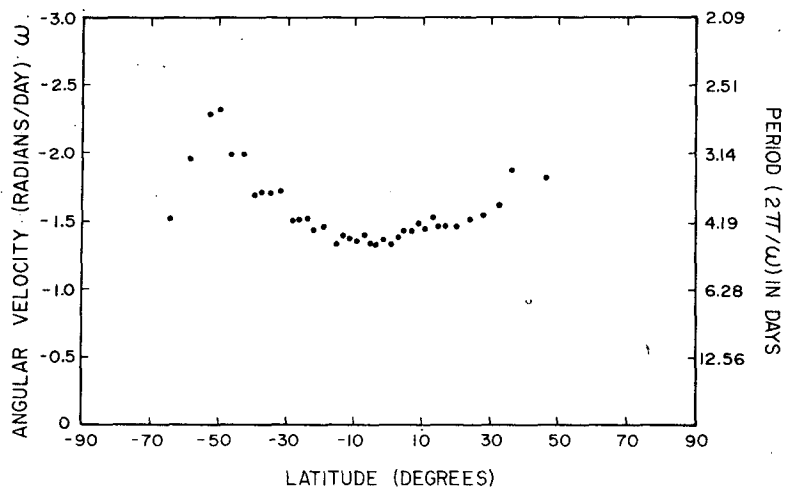


FIG. 10. Latitudinal profile of the angular velocity of the UV features about the axis of rotation of the planet.

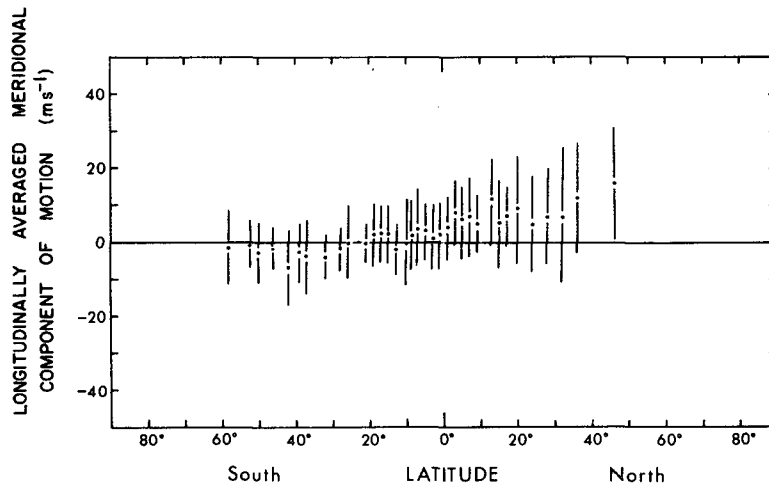


FIG. 11. Latitudinal profile of the space-time-averaged meridional component of motion of the UV features.

latitude from its equatorial value. Indeed, the latitudinal shear of the motions may be better seen in terms of angular velocity about the rotation axis of the planet, as shown in Fig. 10. Peak rotation speeds corresponding to a period of less than 3 days are evident at $\sim 50^\circ$ latitude south, with longer periods on either side, thus constituting a "jet stream". Note that the latitude band between $30\text{--}38^\circ$ latitude south shows four points with same angular speed, or corotation in that band. Note that Fig. 13 shows that the horizontal angular momentum transport into that band is very small.

The zonal average meridional profile of the meridional component of motion shows (Fig. 11) that the mean meridional motion at all latitudes in the northern hemisphere is directed towards the northern Venus pole. The mean flow in the southern hemisphere is equatorward up to $\sim 22^\circ$ latitude and toward the southern pole at higher southerly latitudes. It can be also seen that the mean meridional component meridional profile is not symmetric about the equator—the magnitudes are greater in the northern hemisphere than in the southern hemisphere at the same latitudes. Further, the variability in the meridional component is greater than the zonal mean value at most latitudes. Part of this is definitely real, and some part is very likely due to limiting resolution of the images. Note that the expected error in tracking is $\sim 5\text{--}6\text{ m s}^{-1}$, comparable to the meridional component itself. Ideally, if one wanted to measure the meridional component with a greater accuracy, higher resolution images would need to be used. Unfortunately, the combination of the image resolutions and the prevalent magnitude of zonal component preclude any reduction in uncertainty in the meridional component with the technique and the data used in this study.

5. Discussion

a. Reproducibility of the results

The results presented here are in qualitative and quantitative agreement with those presented by Suomi (1974) and confirm the reproducibility of the ultraviolet feature motions determined from the Mariner 10 images. The differences between the previous results and those presented here are due to slightly different goals in the analysis. Whereas the emphasis in the previous cases was to quantify the motions of several target clouds over the visible disk, that in the present case was to perform a more systematic study of the large scale cloud motions over as much of the Venus globe as possible. Thus, Suomi (1974) presented meridional profiles of target averages, and we present here the spatially averaged profiles. Had the number of targets in the previous study been greater, there would essentially be no difference in the interpretation of the analysis and results.

Travis (1978) has also presented a latitudinal profile of the angular velocity obtained from tracking of large scale ultraviolet clouds in 8 Mariner 10 ultraviolet images of Venus, which is essentially in agreement with the one obtained from the time-space mean latitudinal profile of the zonal component of motion of ultraviolet features.

b. Barotropic instability: Absolute vorticity profile

The jet structure seen in the time mean zonally averaged latitudinal profile of the zonal component of motion is suggestive of barotropically unstable motions (Kuo, 1951) in the Venus atmosphere. Travis (1978) has shown that the mean zonal "wind" profile from his cloud tracking is barotropically unstable

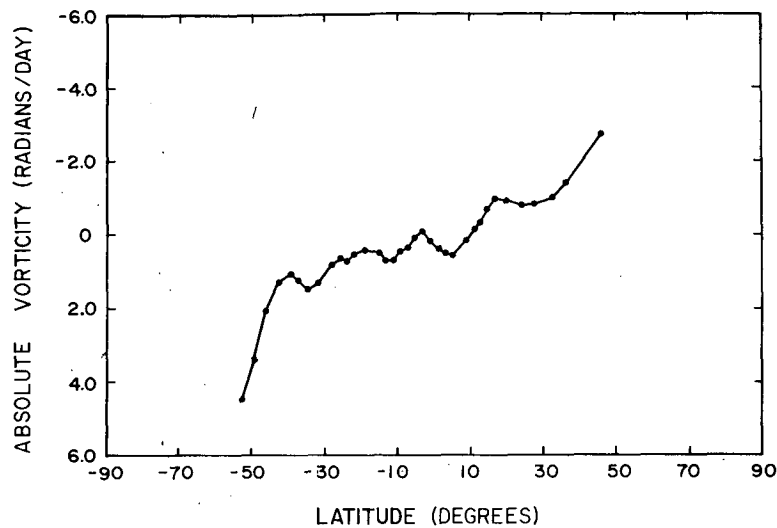


FIG. 12. Latitudinal profile of the absolute vorticity corresponding to the mean zonal component profile shown in Fig. 11.

at $\sim 48^\circ$ latitude (averaged over both hemispheres). Further, he finds that the disturbances with wave-number 7 have maximum amplification rates. According to the Rayleigh criterion the zonally averaged profile may indicate barotropic instability if the absolute vorticity is an extremum somewhere within the flow. The profile of absolute vorticity obtained from the space-time-averaged latitudinal profile of the zonal component of motion alone is shown in Fig. 12. It is seen that the absolute vorticity profile with latitude shows locally extreme values at $\sim 43^\circ$ and 35° latitude in the southern hemisphere and possibly at $\sim 25^\circ$ north latitude. The equatorial region shows some smaller extreme values, although their presence is probably due to noise. Poleward of 43° south and 30° north latitudes the absolute vorticity increases and lack of data precludes inference of whether extreme values are reached. The absolute vorticity profile obtained here is somewhat different from that obtained by Travis (1978). He obtained a well-defined extreme value at 48° latitude ($4.5 \text{ radians day}^{-1}$), whereas our computations show magnitude of the absolute vorticity as computed for the mean profile of Fig. 9, to be less than $1.5 \text{ radians day}^{-1}$ between 43° south and 33° north latitudes and greater poleward of these limits.

The disagreement is due to differences in (i) the precise shape of the meridional profile of the zonal component, and (ii) the time-averaging implicit in the present case. The relative vorticity is dominated by the shear term in mid- and high latitudes; hence, slight differences in the mean meridional profile of the zonal component can produce large differences in the meridional vorticity profile.

Whether or not an instability condition exists on

Venus depends on the degree of barotropy, about which we have little information. In other words, if the pressure and density surfaces do not coincide, then the horizontal flow would vary with height and then it is the profile of potential vorticity that would determine the stability or the instability of the mean zonal flow toward disturbances. The existence of such an instability cannot be established with confidence from Fig. 12.

c. General circulation: Angular momentum transport

We know that at least at the time of Mariner 10 encounter with Venus the upper atmosphere of Venus was organized into two giant circumpolar, hemispheric vortices as evidenced by the global organization of the ultraviolet features (Suomi and Limaye, 1978). The results presented here support such an organization at the cloud-top levels. The vortex circulation is characterized by a weak mean meridional flow directed toward the center of the circulation, and is expected to be responsible for transporting zonal angular momentum towards higher latitudes.

General circulation on Venus would have to be maintained by some process that redistributes the solar energy absorbed globally by the planet. Atmospheric motions that perform this task will also redistribute angular momentum in the atmosphere and contribute to the maintenance of the rapid retrograde circulation of the upper atmosphere. There have been suggestions that a Hadley-type circulation between the equator and the poles may play a significant part in the maintenance of the Venus atmospheric motions (Leovy, 1973; Murray *et al.*, 1974; Suomi, 1974; Gierasch, 1975). It is thus of considerable interest to determine the strength of

such a mean meridional circulation in the atmosphere of Venus.

While we have no direct information about the depth through which the observed ultraviolet feature motions persist (at the very least, they extend at least one scale height deeper than the unit optical depth in the ultraviolet, that, according to Kawabata and Hansen (1975) occurs at ~ 50 mb level), we can estimate the relative meridional transport of angular momentum. Note that due to the lack of any thermal observations no computation of heat transports is possible.

The departure of the meridional profile of the longitudinally averaged zonal component of motion from the constant angular velocity profile is compelling evidence for horizontal angular momentum transports either by a mean meridional circulation or by large scale horizontal eddies, or by both. Whether the mean meridional circulation or the eddy circulation is dominant is certainly of importance in understanding the dynamics of the upper atmosphere of Venus, but determining their relative magnitudes reliably is difficult. Nevertheless, we cannot resist the temptation to calculate the relative contributions to the poleward transport of angular momentum at the cloud-top level by the mean circulation and the transient eddies. Note that since we do not know the depth of the circulation, it is not possible to compute the vertically integrated transport across latitude circles, but only the terms $\langle U \rangle \langle V \rangle$ and $\langle u'v' \rangle$, wherein $\langle U \rangle$ and $\langle V \rangle$ are the zonal mean values of the zonal and meridional components of motion, u' and v' are the observed deviations from the zonal mean values $\langle U \rangle$ and $\langle V \rangle$ respectively, and $\langle u'v' \rangle$ the average covariance. In order to compute these, the measured vectors were binned into approximately 10° latitude bands (so that a sufficiently high number of vectors was available in each band to calculate the covariances), and the longitudinal averages of the zonal and meridional components of motion were calculated along with the covariance $u'v'$. The terms $\langle U \rangle \langle V \rangle$ and $\langle u'v' \rangle$, which are, respectively, the relative contributions to poleward angular momentum by the mean and the eddy circulations (cf. Lorenz, 1967), are shown in Fig. 13. Except at extreme latitudes, the mean circulation appears to dominate over the eddy circulation in the angular momentum transport. The transports at high latitudes ($>45^\circ$ latitude) are somewhat uncertain due to the paucity of reliable measurements since the mean zonal and meridional components have greater error. Note also that the mean poleward angular momentum transport depicted in Fig. 13 differs slightly from a profile obtained directly from the meridional profiles of mean u and v components (Figs. 9 and 11, respectively) due to (i) the inclusion of "abnor-

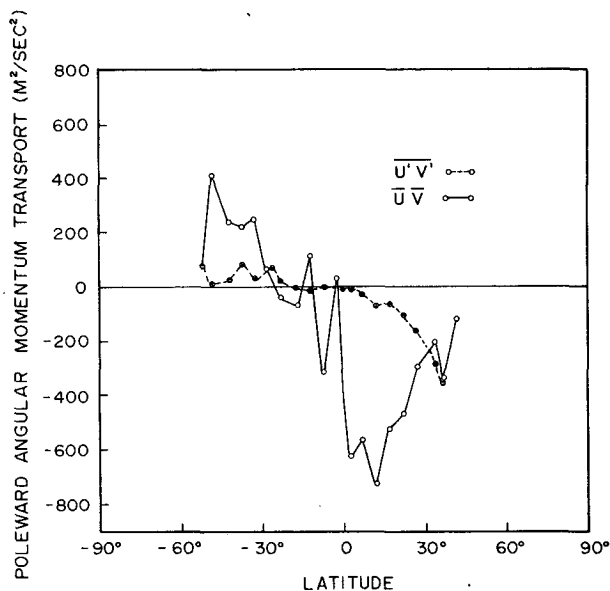


FIG. 13. Relative contribution to the poleward angular momentum transport by the mean circulation ($\langle U \rangle \langle V \rangle$) and by the eddy circulation ($\langle u'v' \rangle$), as a function of latitude.

mal" vectors that were suspected to be indicative of wave motion and were excluded in obtaining longitudinal mean profiles of u and v components; and, (ii) the different width of the latitudinal averaging interval, 10° versus 2° . Nevertheless, the differences show up only when the number of measurements in a latitude band is small, e.g., north of $\sim 25^\circ$ latitude. These results should only be taken as somewhat tentative due to the limited time coverage of the data. More extensive imaging coverage, such as that being gathered from the Pioneer Venus Mission, is needed to determine these terms with better confidence.

6. Some recent results from Pioneer Venus Missions

Recently, some results on the motions in the atmosphere of Venus have been obtained from the Pioneer Venus Multiprobe and Orbiter Missions that are relevant to those reported here. Specifically, Counselman *et al.* (1979, 1980) have obtained altitude profiles of the horizontal components of the wind by tracking of the entry probes. While the results reported so far extend only up to 60 km above the surface, all three profiles presented by them (30°N , 30°S and 59°N), show zonal speeds exceeding 90 m s^{-1} retrograde above 58 km altitude. In addition, the high latitude profile shows a faster zonal component than the midlatitude profiles at all altitudes above 35 km, thus suggesting increase of zonal speed with latitude at those altitudes. Tracking of ultraviolet clouds in the Orbiter Cloud Photo-

polarimeter (OCP) images (S.S.L. is engaged in this task presently) so far shows the existence of ~ 100 m s⁻¹ winds in the same retrograde sense at the cloud level, although the midlatitude jet evidenced in Mariner 10 data appears to be absent, and instead a weak low-latitude jet in the northern hemisphere is seen. The mean meridional component of motion in both the hemispheres is poleward directed in these results as in the case of Mariner 10 results (Rossow *et al.*, 1980).

7. Summary

The time mean (over the duration of Mariner 10 observing period) meridional profile of the zonal component of the motions of the ultraviolet features shows evidence of jet cores at midlatitudes in both the hemispheres. The latitude of the zonal component maximum appears to vary somewhat with time, although a precise time history is not possible because of lack of sufficient data. The mean meridional component of motion is much smaller than the zonal component of motion, and is poleward directed in either hemisphere at most latitudes.

Objective analysis of the velocity measurements yields a "time mean" motion field at the cloud level and shows organized structure on planetary and smaller spatial scales. Well-defined jet maxima are evident as are regions of relatively low velocities. The flow field is largely zonal and suggests the presence of atmospheric waves.

An attempt was made to determine the relative strengths of the mean and eddy circulation, and the tentative conclusion is that the mean circulation is the dominant mode in poleward transport of angular momentum.

The observation period from Mariner 10 was limited to ~ 8 days, and only the images from the first 3–4 days are usable for feature tracking. The results presented here are thus characteristic of that period only. We have discerned some temporal variability, and it would be interesting to determine it more precisely. The data from the Pioneer Venus Orbiter Mission is ideal in this respect due to its long life, and it is hoped that analysis of that data will enhance our knowledge of the dynamics of the Venus atmosphere.

Finally, we have not addressed the question of the dependence of the cloud velocities on their size. Terrestrial experience shows that the smaller the cloud the smaller the difference between its motion and the ambient wind. Storm systems generally do not move with the ambient wind. Extension of this experience to Venus will imply a scale dependence of motions also. The mean zonal speed obtained by Travis by tracking much larger features (about 8 times the spatial scale of those used in this study

or roughly 50–70 times greater area) are slower than those presented here. Unfortunately, it is not possible to extend this to smaller scales because of the poor contrasts in the images. Nevertheless, until the scale dependence of motions has been firmly established, interpretations of the measurements of motions must be done with caution.

Acknowledgments. This research was sponsored by NASA under Grant NGR 50-002-189 from the Planetary Programs Office. This paper is largely based on the thesis submitted by S.S.L. to the Department of Meteorology, University of Wisconsin–Madison, and was revised while S.S.L. was supported by the National Research Council as a Resident Research Associate at the Institute for Space Studies, Goddard Space Flight Center, New York.

We acknowledge the support and cooperation of numerous people at the Jet Propulsion Laboratory, Pasadena, and the Space Science and Engineering Center at the University of Wisconsin–Madison. In particular we wish to thank Mr. Robert J. Krauss and Mrs. Vita Epps. We would also like to thank Prof. Conway Leovy for reviewing this paper and for his helpful comments.

REFERENCES

- Anderson, J. L., M. J. S. Belton, G. E. Danielson, N. Evans and J. M. Soha, 1978: Venus in motion. *Astrophys. J.* (Suppl. Ser.), **36**, 275–284.
- Belton, M. J. S., G. Schubert and A. D. Del Genio, 1976b: Cloud patterns, waves and convection in the Venus atmosphere. *J. Atmos. Sci.*, **33**, 1394–1417.
- Boyer, C., and P. Guerin, 1969: Etude de la rotation retrograde, en 4 jours, de la couche exterior nuageuse de Venus. *Icarus*, **11**, 338–355.
- Caldwell, J., 1972: Retrograde rotation of the upper atmosphere Venus. *Icarus*, **17**, 608–616.
- Chatters, G. C., and V. E. Suomi, 1975: The application of McIDAS. *IEEE Trans. Geosci. Electron.*, **GE-13**, 137–146.
- Counselman III, C. C., S. A. Gourevitch, R. W. King, G. B. Lorient and R. G. Prinn, 1979: Venus winds are zonal and retrograde below the clouds. *Science*, **205**, 85–87.
- , —, —, — and E. S. Ginsberg, 1980: Zonal and meridional circulation of the lower atmosphere of Venus determined by radio interferometry. *J. Geophys. Res.*, **85**, 8026–8030.
- Dunne, J. A., 1974: Mariner 10 Venus encounter. *Science*, **183**, 1289–1291.
- Gierasch, P. J., 1975: Meridional circulation and the maintenance of the Venus atmospheric rotation. *J. Atmos. Sci.*, **32**, 1038–1044.
- Kawabata, K., and J. E. Hansen, 1975: Interpretation of polarization over the disk of Venus. *J. Atmos. Sci.*, **32**, 1133–1139.
- Kuo, H. L., 1951: Dynamical aspects of the general circulation and the stability of the zonal flow. *Tellus*, **3**, 268–284.
- Leovy, C., 1973: Rotation of the upper atmosphere of Venus. *J. Atmos. Sci.*, **28**, 1218–1220.
- Limaye, S. S., 1977: Global scale inertial oscillations on Venus. *Bull. Amer. Astron. Soc.*, **9**, 467.
- , and V. E. Suomi, 1977: Possible detection of an atmospheric wave on Venus. *Bull. Amer. Astron. Soc.*, **9**, 509.
- Lorenz, E. N., 1967: The nature and theory of the general cir-

- ulation of the atmosphere. World Meteorological Organization, 161 pp.
- Murray, B. C., M. J. S. Belton, G. E. Danielson, M. E. Davies, D. Gault, B. Hapke, B. O'Leary, R. Strom, V. Suomi and N. Trask, 1974: Venus: Atmospheric motion and structure from Mariner 10 pictures. *Science*, **183**, 1307-1315.
- Rossow, W. B., and G. P. Williams, 1979: Large-scale motion in the Venus stratosphere. *J. Atmos. Sci.*, **36**, 377-389.
- , A. D. Del Genio, S. S. Limaye, L. D. Travis and P. H. Stone, 1980: Cloud morphology and motions from Pioneer Venus images. *J. Geophys. Res.*, **85**, 8107-8128.
- Smith, E. A., 1975: The McIDAS System. *IEEE Trans. Geosci. Electron.*, **GE-13**, 123-126.
- , and D. R. Phillips, 1975: Automated cloud tracking using precisely aligned digital ATS pictures. *IEEE Trans. Comput.*, **C-21**, 715-729.
- Suchman, D. R., and D. W. Martin, 1976: Wind sets from SMS images: An assessment of quality for GATE. *J. Appl. Meteor.*, **15**, 1266-1278.
- Sidi, C., 1976: Stereoscopic observations of winds on Venus. *Icarus*, **28**, 359-366.
- Smith, B., 1967: Rotation of Venus-continuing contradictions. *Science*, **158**, 114-116.
- Suomi, V. E., and S. S. Limaye, 1978: Venus: Further evidence of vortex circulation. *Science*, **201**, 1009-1011.
- Traub, W. A., and N. P. Carleton, 1975: Spectroscopic observations of winds on Venus. *J. Atmos. Sci.*, **32**, 1045-1059.
- , and —, 1979: Retrograde winds on Venus: Possible periodic variations. *Astrophys. J.*, **227**, 329-333.
- Travis, L. D., 1975: On the origin of ultraviolet contrasts on Venus. *J. Atmos. Sci.*, **32**, 1190-1200.
- , 1978: Nature of the atmospheric dynamics on Venus from power spectrum analysis of Mariner 10 images. *J. Atmos. Sci.*, **35**, 1584-1595.